

# A Manifold Proximal Linear Method for Sparse Spectral Clustering with Application to Single-Cell RNA Sequencing Data Analysis\*

Zhongruo Wang<sup>†</sup>, Bingyuan Liu<sup>‡</sup>, Shixiang Chen<sup>§</sup>, Shiqian Ma<sup>†</sup>, Lingzhou Xue<sup>†</sup>, and Hongyu Zhao<sup>¶</sup>

**Abstract.** Spectral clustering is one of the fundamental unsupervised learning methods widely used in data analysis. Sparse spectral clustering (SSC) imposes sparsity to the spectral clustering and it improves the interpretability of the model. This paper considers a widely adopted model for SSC, which can be formulated as an optimization problem over the Stiefel manifold with nonsmooth and nonconvex objective. Such an optimization problem is very challenging to solve. Existing methods usually solve its convex relaxation or need to smooth its nonsmooth part using certain smoothing techniques. In this paper, we propose a manifold proximal linear method (ManPL) that solves the original SSC formulation. We also extend the algorithm to solve the multiple-kernel SSC problems, for which an alternating ManPL algorithm is proposed. Convergence and iteration complexity results of the proposed methods are established. We demonstrate the advantage of our proposed methods over existing methods via the single-cell RNA sequencing data analysis.

**1. Introduction.** Clustering is a fundamental unsupervised learning problem with wide applications. The hierarchical clustering,  $k$ -means clustering and spectral clustering (SC) methods are widely used in practice [20]. It is known that interpretation of the dendrogram in hierarchical clustering can be difficult in practice, especially for large datasets, and  $K$ -means clustering, closely related to Lloyd’s algorithm, does not guarantee to find the optimal solution and perform poorly for non-linearly separable or non-convex clusters. SC [13, 35, 31] is a graph-based clustering method and it provides a promising alternative for identifying locally connected clusters.

Given the data matrix  $X = [\mathbf{x}_1, \dots, \mathbf{x}_n] \in \mathbb{R}^{p \times n}$ , where  $n$  is the number of data points and  $p$  is the feature dimension, SC constructs a symmetric affinity matrix  $S = (s_{ij})_{n \times n}$ , where  $s_{ij} \geq 0$  measures the pairwise similarity between two data samples  $\mathbf{x}_i$  and  $\mathbf{x}_j$  for  $i, j = 1, \dots, n$ . Denote diagonal matrix  $D = \text{diag}(d_{11}, \dots, d_{nn})$  with  $d_{ii} = \sum_{j=1}^n s_{ij}$ . The main step of SC is to solve the following eigenvalue decomposition:

$$(1.1) \quad \min_{U \in \mathbb{R}^{n \times C}} \langle UU^\top, L \rangle, \text{ s.t., } U^\top U = I_C,$$

where  $L = I_n - D^{-1/2}SD^{-1/2}$  is the normalized Laplacian matrix,  $I_C$  denotes the  $C \times C$  identity matrix, and  $C$  is the number of clusters. The rows of  $U$  can be regarded as an embedding of the data  $X$  from  $\mathbb{R}^p$  to  $\mathbb{R}^C$ . The cluster assignment is then decided after using a standard clustering method such as the  $K$ -means clustering on the estimated embedding matrix  $\hat{U}$  obtained by solving (1.1). Ideally,  $\hat{U}$  should be a sparse matrix such that  $\hat{U}_{ij} \neq 0$  if

\*The first two authors contributed equally to this paper.

<sup>†</sup>Department of Mathematics, UC Davis.

<sup>‡</sup>Department of Statistics, Penn State University.

<sup>§</sup>Department of Industrial & Systems Engineering, Texas A&M University.

<sup>¶</sup>Department of Biostatistics, Yale University.

and only if the sample  $i$  belongs to the  $j$ -th cluster. Therefore  $\hat{U}\hat{U}^\top$  should be a block diagonal matrix which is also sparse. To this end, the sparse spectral clustering (SSC) [29, 28, 32] is proposed to impose sparsity on  $\hat{U}\hat{U}^\top$ , which leads to the following optimization problem:

$$(1.2) \quad \min_{U \in \mathbb{R}^{n \times c}} \langle UU^\top, L \rangle + \lambda \|UU^\top\|_1, \text{ s.t.}, U^\top U = I_C,$$

where  $\|Z\|_1 = \sum_{ij} |Z_{ij}|$  is the entry-wise  $\ell_1$  norm of  $Z$  that promotes the sparsity of  $UU^\top$ , and  $\lambda > 0$  is a regularization parameter.

In practice, the performance of SSC is sensitive to a single measure of similarity between data points, and there are no clear criteria to choose an optimal similarity measure. Moreover, for some very complex data such as the single-cell RNA sequencing (scRNA-seq) data [24], one may benefit from considering multiple similarity matrices because they provide more information to the data. The next-generation sequencing technologies provide large detailed catalogs of the transcriptomes of massive cells to identify putative cell types. Clustering high-dimensional scRNA-seq data provides an informative step to disentangle the complex relationship between different cell types. For example, it is important to characterize the patterns of monoallelic gene expression across mammalian cell types [14], explore the mechanisms that control the progression of lung progenitors across distinct cell types [39], or study the functionally distinct lineage in the bone marrow across mouse conventional dendritic cell types [34]. To this end, Park and Zhao [32] suggest the following similarity matrices which lead to multiple-kernel SSC (MKSSC):

$$K_{\sigma, m}(i, j) = \exp\left(\frac{\|\mathbf{x}_i - \mathbf{x}_j\|^2}{2\epsilon_{ij}^2}\right), \epsilon_{ij} = \frac{\sigma(\mu_i + \mu_j)}{2}, \mu_i = \frac{\sum_{\ell \in \text{KNN}(i)} \|\mathbf{x}_i - \mathbf{x}_\ell\|}{m},$$

where  $\text{KNN}(i)$  represents a set of sample indices that are the top  $m$  nearest neighbors of the sample  $\mathbf{x}_i$ . The parameters  $\sigma$  and  $m$  control the width of the neighborhoods. We use  $S(\sigma)$  and  $S(m)$  to denote the sets of possible choices of  $\sigma$  and  $m$ , respectively. Then the total number of similarity matrices is equal to  $T = |S(\sigma)| \cdot |S(m)|$ . We denote the normalized Laplacian matrices corresponding to these  $T$  similarity matrices as  $L^{(\ell)}$ ,  $\ell = 1, \dots, T$ . The MKSSC can be formulated as the following optimization problem:

$$(1.3) \quad \min_{U \in \mathbb{R}^{n \times c}, w \in \mathbb{R}^T} \bar{F}(U, w) \equiv \left\langle UU^\top, \sum_{\ell=1}^T w_\ell L^{(\ell)} \right\rangle + \lambda \|UU^\top\|_1 + \rho \sum_{\ell=1}^T w_\ell \log(w_\ell)$$

$$\text{s.t.} \quad U^\top U = I_C, \sum_{\ell=1}^T w_\ell = 1, w_\ell \geq 0, \ell = 1, \dots, T,$$

where  $w_\ell, \ell = 1, \dots, T$  are unknown weightings of the kernels, and  $\rho \sum_{\ell=1}^T w_\ell \log(w_\ell)$  serves as a regularization term, and  $\lambda, \rho$  are two regularization parameters. Note that  $w_\ell \log(w_\ell)$  yields a closed-form solution of  $w_\ell$  in the iterative algorithm we introduce later, which reduces the computational time.

Note that both SSC (1.2) and MKSSC (1.3) are nonconvex and nonsmooth with Riemannian manifold constraints. Therefore, they are both numerically challenging to solve.

this paper, we propose a manifold proximal linear (ManPL) method for solving the SSC (1.2) in Section 2, and an alternating ManPL (AManPL) method for solving the MKSSC (1.3) in Section 3. ManPL and AManPL enjoy the convergence guarantees for solving the nonsmooth manifold optimization problem. Moreover, we present the numerical experiments in Section 4 to demonstrate the numerical performance of ManPL and AManPL in benchmark datasets, synthetic datasets, and real datasets in single-cell data analysis.

**Our contributions** lie in several folds.

1. We propose ManPL method for solving SSC (1.2) and AManPL method for solving MKSSC (1.3).
2. We analyze the convergence and iteration complexity of both ManPL and AManPL.
3. We apply our proposed methods to clustering of single-cell RNA sequencing data .

**Notation.** Throughout this paper, we use  $\mathcal{M}$  to denote the Stiefel manifold. The smoothness, convexity, and Lipschitz continuity of a function  $f$  are always interpreted as the function is considered in the ambient Euclidean space. We use  $\mathbb{S}_+^n$  to denote the set of  $n \times n$  positive semidefinite matrices,  $\text{Tr}(Z)$  to denote the trace of matrix  $Z$ .

**2. A Manifold Proximal Linear Method for SSC.** Since SSC (1.2) is both nonsmooth and nonconvex, it is numerically challenging to solve. In the literature, convex relaxations and smooth approximations of (1.2) have been suggested. In particular, Lu et. al. [29] proposed to replace  $UU^\top$  with a positive semidefinite matrix  $P$  and solve the following convex relaxation:

$$(2.1) \quad \min_{P \in \mathbb{S}_+^n} \langle P, L \rangle + \lambda \|P\|_1, \text{ s.t., } 0 \preceq P \preceq I, \text{ Tr}(P) = C.$$

This convex problem (2.1) can be solved by classical optimization algorithms such as ADMM. Denote the solution of (2.1) by  $\hat{P}$ , the solution of (1.2) can be approximated by the top  $C$  eigenvectors of  $\hat{P}$ . In another work, Lu et. al. [28] proposed a nonconvex ADMM to solve the following smooth variant of (1.2):

$$(2.2) \quad \min_{U \in \mathbb{R}^{n \times C}, P \in \mathbb{S}_+^n} \langle UU^\top, L \rangle + g(P), \text{ s.t., } P = UU^\top, U^\top U = I_C,$$

where  $g(\cdot)$  is a smooth function that approximates the  $\ell_1$  regularizer  $\lambda \|\cdot\|_1$ . In [28], the authors used the following smooth function:

$$(2.3) \quad g(P) := \max_Z \langle P, Z \rangle - \frac{\sigma}{2} \|Z\|_F^2, \text{ s.t., } \|Z\|_\infty \leq \lambda,$$

where  $\|Z\|_\infty = \max_{ij} |Z_{ij}|$ , and  $\sigma > 0$  is a smoothing parameter. The nonconvex ADMM for solving (2.2) typically iterates as

$$(2.4a) \quad U^{k+1} := \arg \min_{U \in \mathbb{R}^{n \times C}} \mathcal{L}(U, P^k; \Lambda^k), \text{ s.t., } U^\top U = I_C$$

$$(2.4b) \quad P^{k+1} := \arg \min_{P \in \mathbb{S}_+^n} \mathcal{L}(U^{k+1}, P; \Lambda^k),$$

$$(2.4c) \quad \Lambda^{k+1} := \Lambda^k - \mu(P^{k+1} - U^{k+1}U^{k+1\top}),$$

where the augmented Lagrangian function  $\mathcal{L}$  is defined as

$$\mathcal{L}(U, P; \Lambda) := \langle UU^\top, L \rangle + g(P) - \langle \Lambda, P - UU^\top \rangle + \frac{\mu}{2} \|P - UU^\top\|_F^2,$$

and  $\mu > 0$  is a penalty parameter. The two subproblems (2.4a) and (2.4b) are both relatively easy to solve. The reason to use the smooth function  $g(\cdot)$  to approximate  $\lambda \|\cdot\|_1$  in (2.2) is for the purpose of convergence guarantee. In [28], the authors proved that any limit point of the sequence generated by the nonconvex ADMM (2.4) is a stationary point of (2.2). This result relies on the fact that function  $g$  is smooth. If one applies ADMM for the original SSC (1.2), then no convergence guarantee is known.

Note that both the convex relaxation (2.1) and the smooth approximation (2.2) are only approximations to the original SSC (1.2). In this section, we introduce our ManPL algorithm that solves the original SSC (1.2) directly. For the ease of presentation, we rewrite (1.2) as

$$(2.5) \quad \min_U F(U) \equiv f(U) + h(c(U)), \text{ s.t., } U \in \mathcal{M},$$

where  $f(U) = \langle UU^\top, L \rangle$ ,  $h(\cdot) = \lambda \|\cdot\|_1$ ,  $c(U) = UU^\top$ ,  $\mathcal{M} = \{U \in \mathbb{R}^{n \times C} \mid U^\top U = I_C\}$  is the Stiefel manifold. Moreover, note that  $f$  and  $c$  are smooth mappings, and  $h$  is nonsmooth but convex in the ambient Euclidean space. Therefore, (2.5) is a Riemannian optimization problem with nonsmooth objective. Furthermore, throughout this paper, we use  $L_f$ ,  $L_c$ ,  $L_h$  to denote the Lipschitz constants of  $\nabla f$ ,  $\nabla c$ , and  $h$ , respectively. Riemannian optimization has drawn much attention recently, due to its wide applications, including low rank matrix completion [4], phase retrieval [2, 37], phase synchronization [3, 27], and dictionary learning [12, 36]. Several important classes of algorithms for Riemannian optimization with a smooth objective function were covered in one monograph [1]. On the other hand, there has been limited number of algorithms for Riemannian optimization with nonsmooth objective until very recently. The most natural idea for this class of optimization problems is the Riemannian subgradient method (RSGM) [19, 21, 23]. Recently, Li et. al. [26] studied the RSGM for Riemannian optimization with weakly convex objective. In particular, they showed the number of iteration needed by RSGM for obtaining an  $\epsilon$ -stationary point is  $O(\epsilon^{-4})$ . Motivated by the proximal gradient method for solving composite minimization in Euclidean space, Chen et. al. [10] proposed a manifold proximal gradient method (ManPG) for solving the following Riemannian optimization problem that includes the sparse PCA [43] as a special example:

$$(2.6) \quad \min_X f(X) + h(X), \text{ s.t., } X \in \mathcal{M},$$

where  $\mathcal{M}$  is the Stiefel manifold,  $f$  is a smooth function, and  $h$  is a nonsmooth and convex function. The iteration complexity of ManPG is proved to be  $O(\epsilon^{-2})$  for obtaining an  $\epsilon$ -stationary point [10], which is better than the complexity of RSGM [26]. Variants of ManPG have been designed for different applications, such as alternating ManPG (A-ManPG) [11] for sparse PCA and sparse CCA, manifold proximal point algorithm (ManPPA) [8, 9] for robust subspace recovery and orthogonal dictionary learning, and stochastic ManPG [40] for online sparse PCA. Motivated by the success of ManPG and its variants, we propose a manifold proximal linear algorithm for solving SSC (2.5).

The proximal linear method has recently drawn great research attentions. It targets to solve the optimization problem in the form of (2.5) without the manifold constraint, i.e.,

$$(2.7) \quad \min_{x \in \mathbb{R}^n} f(x) + h(c(x)),$$

where  $f : \mathbb{R}^n \rightarrow \mathbb{R}$  and  $c : \mathbb{R}^n \rightarrow \mathbb{R}^m$  are smooth mappings,  $h : \mathbb{R}^m \rightarrow \mathbb{R}$  is convex and nonsmooth. The proximal linear method for solving (2.7) iterates as follows:

$$(2.8) \quad x^{k+1} := \arg \min_x \langle \nabla f(x^k), x - x^k \rangle + h(c(x^k)) + J(x^k)(x - x^k) + \frac{1}{2t} \|x - x^k\|_2^2,$$

where  $J(x) = \nabla c(x)$  is the Jacobian of  $c$ , and  $t > 0$  is a step size. Note that since  $h$  is convex, the update (2.8) is a convex problem. This method has been studied recently by [25, 15, 18] and applied to solving many important applications such as robust phase retrieval [17], robust matrix recovery/completion [6], and robust blind deconvolution [7].

Due to the nonconvex constraint  $U \in \mathcal{M}$ , solving (2.5) is more difficult than (2.7). Motivated by ManPG and the proximal linear method (2.8), we propose a ManPL algorithm for solving (2.5). A typical iteration of the ManPL algorithm for solving (2.5) is:

$$(2.9a) \quad V^k := \arg \min_V \langle \nabla f(U^k), V \rangle + h(c(U^k)) + J(U^k)V + \frac{1}{2t} \|V\|_F^2, \text{ s.t., } V \in \mathbb{T}_{U^k} \mathcal{M}$$

$$(2.9b) \quad U^{k+1} := \text{Retr}_{U^k}(\alpha_k V^k),$$

where  $\mathbb{T}_U \mathcal{M}$  denotes the tangent space of  $\mathcal{M}$  at  $U$ ,  $t > 0$  and  $\alpha_k > 0$  are step sizes, and  $\text{Retr}$  denotes the retraction operation. For Stiefel manifold,  $\mathbb{T}_U \mathcal{M} := \{V \mid V^\top U + U^\top V = 0\}$  and in this paper we choose the retraction operation to be the one based on the Polar decomposition (see more details in Appendix A). The equation (2.9a) computes the descent direction  $V$  by minimizing a convex function over the tangent space of  $\mathcal{M}$ . The objective function is a linearization of the smooth functions  $f$  and  $c$ , plus a quadratic proximal term. The difference of (2.9a) and (2.8) is the constraint in (2.9a), which is needed in the Riemannian optimization setting. The retraction step (2.9b) brings the iterate back to the manifold  $\mathcal{M}$ .

The complete description of the ManPL for solving SSC (2.5) is given in Algorithm 2.1. The step (2.10) is a line search step to find the step size  $\alpha_k$  such that there is a sufficient decrease on the function  $F$ .

The main convergence result of ManPL (Algorithm 2.1) is given as Theorem 2.1. Its proof is given in Appendix B.1.

**Theorem 2.1.** *Assume  $F(U)$  is lower bounded by  $F^*$ . The limit point of the sequence  $\{U^k\}$  generated by ManPL (Algorithm 2.1) is a stationary point of (2.5). Moreover, ManPL returns an  $\epsilon$ -stationary point of (2.5) in  $O(\epsilon^{-2})$  iterations.*

**3. An Alternating ManPL Method for Multiple-Kernel SSC.** In this section, we consider the multiple-kernel SSC (1.3). Park and Zhao [32] consider to solve the following relaxation

---

**Algorithm 2.1** The ManPL for SSC (2.1)

---

Input: initial point  $U^0 \in \mathcal{M}$ , step size  $t > 0$ , parameter  $\beta \in (0, 1)$

**for**  $k = 0, 1, \dots$  **do**

    Calculate  $V^k$  by solving (2.9a)

    Let  $j_k$  be the smallest nonnegative integer such that

$$(2.10) \quad F(\text{Retr}_{U^k}(\beta^{j_k} V^k)) \leq F(U^k) - \frac{\beta^{j_k}}{2t} \|V^k\|_F^2$$

    Let  $\alpha_k = \gamma^{j_k}$  and compute  $U^{k+1}$  by (2.9b)

**end for**

---

of (1.3) by letting  $P = UU^\top$ :

$$(3.1) \quad \min_{P, w} \left\langle P, \sum_{\ell=1}^T w_\ell L^{(\ell)} \right\rangle + \lambda \|P\|_1 + \rho \sum_{\ell=1}^T w_\ell \log(w_\ell)$$

$$\text{s.t. } \text{Tr}(P) = C, 0 \preceq P \preceq I, \sum_{\ell=1}^T w_\ell = 1, w_\ell \geq 0, \ell = 1, \dots, T.$$

Park and Zhao [32] suggested to use an alternating minimization algorithm (AMA) to solve (3.1). Note that this method is named MPSSC in [32]. In the  $k$ -th iteration of AMA, one first fixes  $w$  as  $w^k$  and solves the resulting problem with respect to  $P$  to obtain  $P^{k+1}$ , and then fixes  $P$  as  $P^{k+1}$  and solves the resulting problem with respect to  $w$ . In particular, when  $w$  is fixed as  $w^k$ , problem (3.1) reduces to

$$(3.2) \quad \min_P \left\langle P, \sum_{\ell=1}^T w_\ell^k L^{(\ell)} \right\rangle + \lambda \|P\|_1, \text{ s.t.}, \text{Tr}(P) = C, 0 \preceq P \preceq I,$$

which is a convex problem and can be solved via convex ADMM algorithm. When  $P$  is fixed as  $P^{k+1}$ , problem (3.1) reduces to

$$(3.3) \quad \min_w c^\top w + \rho \sum_{\ell=1}^T w_\ell \log(w_\ell), \text{ s.t.}, \sum_{\ell=1}^T w_\ell = 1, w_\ell \geq 0, \ell = 1, \dots, T,$$

where  $c_\ell = \langle P^{k+1}, L^{(\ell)} \rangle$ ,  $\ell = 1, \dots, T$ . This is also a convex problem and it can be easily verified that (3.3) admits a closed-form solution given by

$$(3.4) \quad w_\ell = \frac{\exp(-c_\ell/\rho)}{\sum_{j=1}^T \exp(-c_j/\rho)}, \ell = 1, \dots, T.$$

In summary, a typical iteration of the AMA algorithm proposed by Park and Zhao [32] is as follows:

$$(3.5) \quad \begin{cases} \text{update } P^{k+1} \text{ by solving (3.2)} \\ \text{update } w^{k+1} \text{ by solving (3.3).} \end{cases}$$

Another approach to approximate (1.3) is to combine the idea of AMA (3.5) and the nonconvex ADMM for solving the smooth problem (2.2). In particular, one can solve the following smooth variant of (1.3):

$$(3.6) \quad \begin{aligned} \min_{U \in \mathbb{R}^{n \times C}, w \in \mathbb{R}^T} \quad & \left\langle UU^\top, \sum_{\ell=1}^T w_\ell L^{(\ell)} \right\rangle + g(UU^\top) + \rho \sum_{\ell=1}^T w_\ell \log(w_\ell) \\ \text{s.t.} \quad & U^\top U = I_C, \sum_{\ell=1}^T w_\ell = 1, w_\ell \geq 0, \ell = 1, \dots, T, \end{aligned}$$

where  $g(\cdot)$  is the smooth approximation to  $\lambda \|\cdot\|_1$  defined in (2.3). When fixing  $w$ , (3.6) is in the same form as the smoothed SSC (2.2), so it can be solved by the nonconvex ADMM (2.4). When fixing  $U$ , (3.6) is in the same form as (3.3), and admits a closed-form solution (3.4). In summary, the AMA+ADMM algorithm for solving (3.6) works as follows:

$$(3.7) \quad \begin{cases} \text{update } U^{k+1} \text{ by solving (3.6) with } w \text{ fixed as } w^k \text{ using nonconvex ADMM (2.4)} \\ \text{update } w^{k+1} \text{ by solving (3.6) with } U \text{ fixed as } U^{k+1} \text{ using (3.4).} \end{cases}$$

By exploiting the structure of (1.3), we propose to solve (1.3) by an alternating ManPL algorithm (AManPL). More specifically, in the  $k$ -th iteration of AManPL, we first fix  $w$  as  $w^k$ , then (1.3) reduces to

$$(3.8) \quad \min_U \left\langle UU^\top, \sum_{\ell=1}^T w_\ell^k L^{(\ell)} \right\rangle + \lambda \|UU^\top\|_1, \text{ s.t., } U \in \mathcal{M},$$

which is in the same form of (2.5) with  $L$  in (2.5) replaced by  $\bar{L} := \sum_{\ell=1}^T w_\ell^k L^{(\ell)}$ . Therefore, (3.8) can also be solved by ManPL. Here we adopt one step of ManPL, i.e., (2.9) to obtain  $U^{k+1}$ . More specifically,  $U^{k+1}$  is computed by the following two steps:

$$(3.9a) \quad V^k := \arg \min_V \langle \nabla_U f(U^k, w^k), V \rangle + h(c(U^k) + J(U^k)V) + \frac{1}{2t} \|V\|_F^2, \text{ s.t., } V \in \mathbb{T}_{U^k} \mathcal{M}$$

$$(3.9b) \quad U^{k+1} := \text{Retr}_{U^k}(\alpha_k V^k),$$

where  $f(U, w) := \langle UU^\top, \sum_{\ell=1}^T w_\ell L^{(\ell)} \rangle$ ,  $h(\cdot) := \lambda \|\cdot\|_1$ , and  $c(U) = UU^\top$ . We then fix  $U$  in (1.3) as  $U^{k+1}$ , and then (1.3) reduces to

$$(3.10) \quad \min_w c^\top w + \rho \sum_{\ell=1}^T w_\ell \log(w_\ell), \text{ s.t., } \sum_{\ell=1}^T w_\ell = 1, w_\ell \geq 0, \ell = 1, \dots, T,$$

where  $c_\ell = \langle U^{k+1} U^{k+1 \top}, L^{(\ell)} \rangle$ ,  $\ell = 1, \dots, T$ . This optimization problem has the same form as (3.3), and again admits a closed-form solution given by (3.4). The AManPL is described in Algorithm 3.1.

We have the following convergence and iteration complexity analysis for AManPL for solving MKSSC (1.3). Its proof is given in Appendix B.2.

---

**Algorithm 3.1** The AManPL Method for Solving MKSSC (1.3)

---

Input: initial point  $U^0 \in \mathcal{M}$ , step size  $t > 0$ , parameter  $\beta \in (0, 1)$ , let  $w^0$  be the optimal solution to (3.10) for  $c_\ell = \langle U^0 U^{0\top}, L^{(\ell)} \rangle$

**for**  $k = 0, 1, \dots$  **do**

    Calculate  $V^k$  by solving (3.9a)

    Let  $j_k$  be the smallest nonnegative integer such that

$$(3.11) \quad \bar{F}(\text{Retr}_{U^k}(\beta^{j_k} V^k), w^k) \leq \bar{F}(U^k, w^k) - \frac{\beta^{j_k}}{2t} \|V^k\|_F^2$$

    Let  $\alpha_k = \beta^{j_k}$  and compute  $U^{k+1}$  by (3.9b)

    Update  $w_\ell^{k+1}$  by (3.4) with  $c_\ell = \langle U^{k+1} U^{k+1\top}, L^{(\ell)} \rangle$ ,  $\ell = 1, \dots, T$ .

**end for**

---

**Theorem 3.1.** Assume  $\bar{F}(U, w)$  in (1.3) is lower bounded by  $\bar{F}^*$ . The limit point of the sequence  $\{U^k, w^k\}$  generated by AManPL (Algorithm 3.1) is a stationary point of problem (1.3). Moreover, to obtain an  $\epsilon$ -stationary point, the number of iterations needed by AManPL is  $O(\epsilon^{-2})$ .

**4. Numerical Experiments.** In this section, we compare our proposed methods ManPL and AManPL with some existing methods. In particular, for SSC (1.2), we compare ManPL (Algorithm 2.1) with convex ADMM [29] (denoted by CADMM<sup>1</sup>) for solving (2.1) and non-convex ADMM [28] (denoted by NADMM) for solving (2.2). We also include the spectral clustering (denoted by SC) in the comparison. For MKSSC (1.3), we compare AManPL (Algorithm 3.1) with MPSSC (i.e., AMA+CADMM<sup>2</sup>) [32] and AMA+NADMM (3.7). Default settings of the parameters for the existing methods were adopted. All the algorithms were terminated when the absolute change of the objective value is smaller than  $10^{-5}$ , which indicates that the algorithms was not making much progress.

Problem	Algorithm	Parameters
Convex SSC (2.1)	CADMM [29]	$\lambda = 10^{-4}$
Smoothed SSC (2.2)	NADMM (2.4) [28]	$\lambda = 10^{-4}, \sigma = 10^{-2}$
Original SSC (1.2)	ManPL (Algorithm 2.1)	$\lambda = 10^{-3}$
MKSSC (3.1)	AMA+CADMM (3.5) [32]	$\lambda = 10^{-4}, \rho = 0.2$
Smoothed MKSSC (3.6)	AMA+NADMM (3.7)	$\lambda = 10^{-4}, \rho = 0.2, \sigma = 10^{-2}$
Original MKSSC (1.3)	AManPL (Algorithm 3.1)	$\lambda = 5 \times 10^{-3}, \rho = 1$

Table 1: Algorithms and their parameters

---

<sup>1</sup>codes downloaded from <https://github.com/canyilu/LibADMM/blob/master/algorithms/sparsesc.m>

<sup>2</sup>codes downloaded from <https://github.com/ishspsy/project/tree/master/MPSSC>



**4.1. UCI Datasets.** We first compare the clustering performance of different methods on three benchmark datasets in UCI machine learning repository [16]. We list the parameters used in the algorithms in Table 1. We follow [32] to construct the similarity matrices and record the normalized mutual information (NMI) to measure the performance of the clustering. Note that higher NMI scores indicate better clustering performance. The NMI scores are reported in Table 2. From Table 2 we see that the three algorithms for SSC usually outperform SC, and among the three algorithms for SSC, ManPL usually outperforms the other two methods. We also see that the MKSSC model usually generates higher NMI scores than SSC. Moreover, among all three algorithms for SSC and three algorithms for MKSSC, the AManPL for MKSSC always has the largest NMI score. This indicates the great potential of our AManPL method for solving MKSSC. Moreover, we show the heatmap of  $|UU^\top|$  for the Wine data set in Figure 1. From this figure we see that for SSC, the NADMM and ManPL generate much better results than CADMM in terms of recovering the block matrices, and for MKSSC, the AMA+NADMM and AManPL generate much better results than AMA+CADMM. The heatmap for the other two data sets are similar, so we omit them for brevity.

Datasets	SC	SSC			MKSSC			C
		CADMM	NADMM	ManPL	AMA+CADMM	AMA+NADMM	AManPL	
Wine	0.8650	0.8650	0.8782	0.8782	0.8854	0.8854	<b>0.8926</b>	3
Iris	0.7496	0.7582	0.7582	0.7582	0.7665	0.7601	<b>0.7705</b>	3
Glass	0.3165	0.3418	0.2047	0.3471	0.2656	0.3315	<b>0.3644</b>	6

Table 2: Comparison of the NMI scores on the UCI data sets.

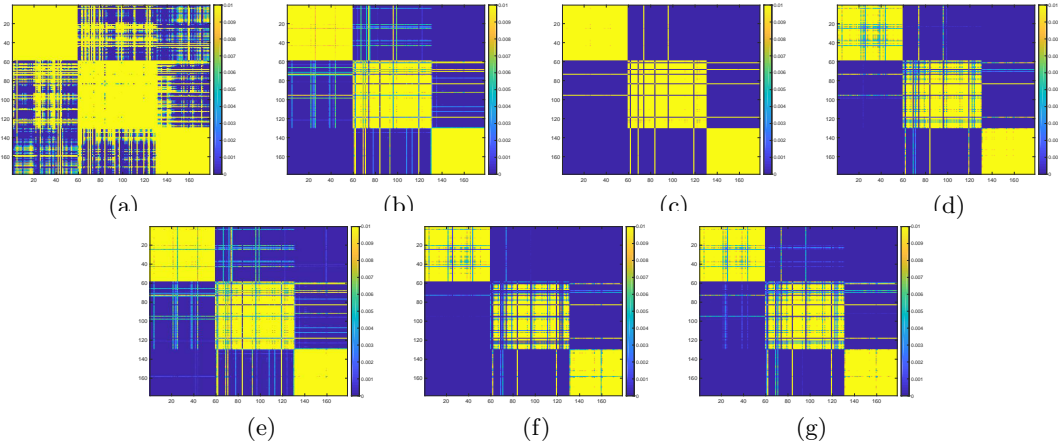


Figure 1: The heatmaps of  $|UU^\top|$  on the Wine dataset estimated by (a) SC, (b) CADMM for SSC, (c) NADMM for SSC, (d) ManPL for SSC, (e) AMA+CADMM for MKSSC, and (f) AManPL for MKSSC.

**4.2. Synthetic Data.** In this subsection, we follow [32] to evaluate the clustering performance of different methods on two synthetic datasets with  $C = 5$  clusters. To compare

ManPL, AManPL and existing methods, we select the regularization parameter  $\lambda$  using an independent tuning dataset and set other parameters as in Table 1. Specifically, we generate the tuning datasets using the same data generating process, and we select the parameter  $\lambda$  that maximizes the average NMI score over 50 independent repetitions. The two synthetic datasets are generated as follows.

- **Synthetic data 1.** We randomly generate  $C$  points in the 2-dimensional latent space spanning a circle as the centers of  $C$  clusters. For each cluster, we randomly generate the points by adding an independent noise to its center. We project these 2-dimensional data to a  $p$ -dimensional space using a linear projection matrix  $P$  and then add the heterogeneous noise  $\epsilon$  to obtain the data matrix  $X$ . The noise level is 30% of the radius of the circle in the embedded space.
- **Synthetic data 2.** We randomly generate a matrix  $B' \in \mathbb{R}^{C \times d}$  with  $d < p$  by drawing its entries independently from the uniform distribution on  $[0, 2]$ . We randomly assign the cluster labels  $z_1, \dots, z_n \in [C]$ . Let  $B = [B', 0_{C \times (p-d)}]$  and  $Z = (Z_{ij})_{n \times C} = (1_{\{z_i=j\}})_{n \times C}$ . We generate  $X = ZB + W$ , where  $W = (W_{ij})_{n \times p}$  is an error matrix with independent normally distributed entries that  $W_{ij} \sim N(0, 0.04)$ .

Figure 2 visualizes one realization of the simulated data for these two settings. From Figure 2 we see that different clusters mix together and the variability between clusters varies. Since we found that MKSSC is better to handle the heterogeneous noise than SSC in both settings, we only focus on the comparison of AMA+CADMM, AMA+NADMM and AManPL for MKSSC. In Table 3, we report the NMI scores of the three algorithms for solving MKSSC, and the NMI scores are averaged over 50 independent runs and the numbers in the parentheses are the standard deviation of the NMI scores. From Table 3 we see that AManPL consistently outperforms the other two methods in all tested instances. This is not surprising because AManPL solves the original MKSSC, and the other two methods only solve its approximations. Moreover, we show the heatmaps of  $|\mathbf{U}\mathbf{U}^\top|$  for synthetic data 1 in Figure 3 (synthetic data 2 is similar). We see that the block diagonal structure is well recovered by AManPL, which shows much better performance than the other two methods.

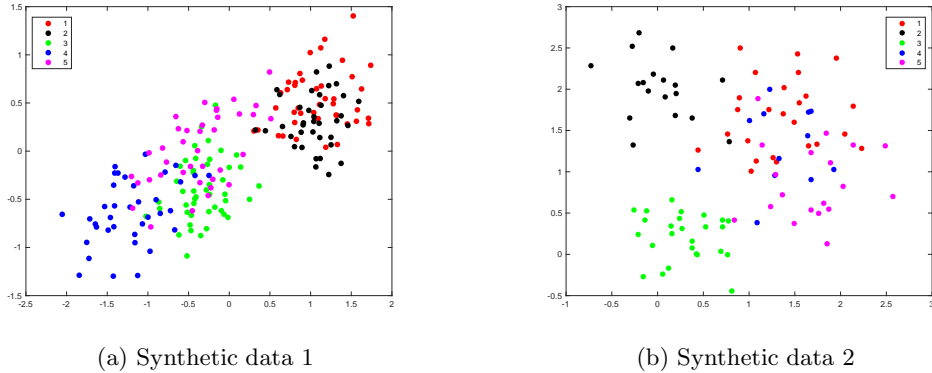


Figure 2: Illustration of one realization of the synthetic data.

Method	AMA+CADMM	AMA+NADMM	AManPL
$n$	$p$	Synthetic data 1	
100	250	0.9852 (1.2e-3)	0.9852 (2.4e-3)
100	300	0.9789 (2.1e-2)	0.9844 (1.4e-2)
100	500	0.9787 (2.0e-3)	0.9834 (1.5e-3)
200	250	0.9821 (1.8e-3)	0.9803 (1.9e-3)
200	300	0.9830 (1.3e-3)	0.9833 (1.3e-3)
200	500	0.9607 (2.8e-3)	0.9606 (2.8e-3)
$n$	$p$	Synthetic data 2	
100	250	0.6491 (5.8e-3)	0.7163 (3.9e-3)
100	300	0.6304 (1.3e-3)	0.7466 (2.4e-3)
100	500	0.6253 (2.3e-3)	0.7289 (1.3e-3)
200	250	0.7977 (2.1e-3)	0.1371 (2.2e-3)
200	300	0.7380 (1.1e-3)	0.1034 (1.2e-3)
200	500	0.7130 (9.6e-3)	0.1220 (2.1e-3)

Table 3: NMI of three algorithms for solving MKSSC for synthetic data.

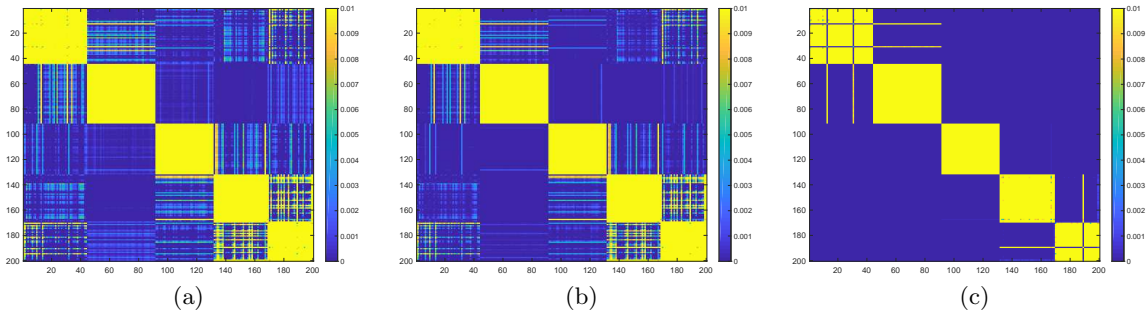


Figure 3: The heatmaps of  $|\mathbf{U}\mathbf{U}^\top|$  on synthetic data 1 estimated by (a) AMA+CADMM, (b) AMA+NADMM, and (c) AManPL for MKSSC.

**4.3. Single-Cell Data Analysis.** Clustering cells and identifying subgroups are important topics in high-dimensional scRNA-seq data analysis. The multiple kernel learning approach is vital as clustering scRNA-seq data is usually sensitive to the choice of the number of neighbors and scaling parameter. Recently, [32] showed that AMA+CADMM for MKSSC provides a promising clustering result and outperforms several state-of-art methods such as SC, SSC, t-SNE [30], and SIMLR [41]. In what follows, we focus on the numerical comparison of AMA+CADMM, AMA+NADMM and AManPL to cluster high-dimensional scRNA-seq data on six real datasets. These six real datasets represent several types of important dynamic processes such as cell differentiation, and they include the information about single cell types. We follow the procedure of [32] to specify multiple kernels for clustering scRNA-seq data and choose the proper tuning parameters  $\lambda$  and  $\rho$ . The six datasets and the NMI scores of the

three algorithms: AMA+CADMM, AMA+NADMM and AManPL for solving MKSSC, are summarized in Table 4. From Table 4 we observe that AManPL always achieves the highest NMI scores and consistently outperforms the other two methods on all six real datasets. We also demonstrate the performance of AManPL by showing the two-dimensional embedding estimated by AManPL in Figure 4. From this table, we see that AManPL yielded clear and meaningful clusters, even for the Ginhoux dataset [34], which was known to be very challenging. This again demonstrates the great practical potential of our AManPL method for analyzing the scRNA-seq data.

Datasets	AMA+CADMM	AMA+NADMM	AManPL	$C$
Deng [14]	0.7319	0.7389	<b>0.7464</b>	7
Ting [38]	0.9283	0.9524	<b>0.9755</b>	5
Treutlein [39]	0.7674	0.7229	<b>0.8817</b>	5
Buettner [5]	0.7929	0.8744	<b>0.8997</b>	3
Ginhoux [34]	0.6206	0.6398	<b>0.6560</b>	3
Pollen [33]	0.9439	0.9372	<b>0.9631</b>	11

Table 4: NMI scores of three algorithms for MKSSC on six real scRNA-seq datasets.

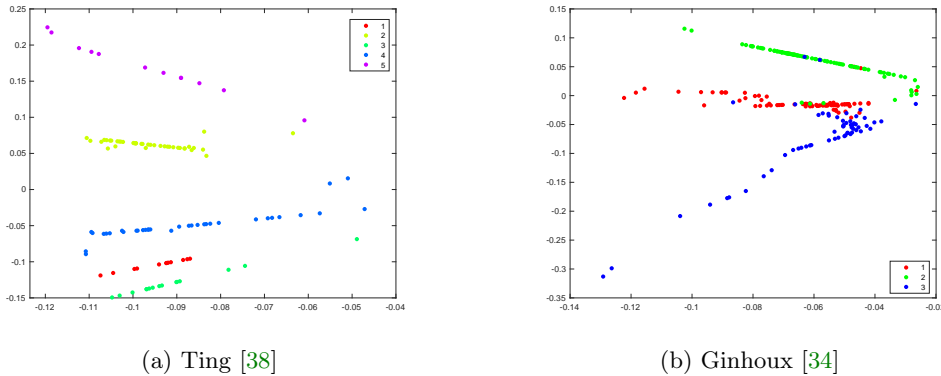


Figure 4: Visualization of the cells in 2-D embedded space using AManPL for MKSSC on two real datasets in high-dimensional scRNA-seq analysis.

**5. Conclusion.** Motivated by the recent need on analyzing single cell RNA sequencing data, we considered the sparse spectral clustering and multiple-kernel sparse spectral clustering in this paper. We proposed the manifold proximal linear method for solving SSC, and the alternating manifold proximal linear method for solving MKSSC. Convergence and iteration complexity of the proposed methods are analyzed. Numerical results on synthetic data and the single cell RNA sequencing data demonstrated the great potential of our proposed methods.

#### Appendix A. Preliminaries.

### A.1. Optimality Condition of Manifold Optimization.

**Definition A.1.** (Generalized Clarke subdifferential [22]) For a locally Lipschitz function  $F$  on  $\mathcal{M}$ , the Riemannian generalized directional derivative of  $F$  at  $X \in \mathcal{M}$  in direction  $V$  is defined by

$$(A.1) \quad F^\circ(X, V) = \limsup_{Y \rightarrow X, t \downarrow 0} \frac{F \circ \phi^{-1}(\phi(Y) + tD\phi(X)[V]) - F \circ \phi^{-1}(\phi(Y))}{t},$$

where  $(\phi, U)$  is a coordinate chart at  $X$  and  $D\phi(X)$  denotes the Jacobian of  $\phi(X)$ . The generalized gradient or the Clarke subdifferential of  $F$  at  $X \in \mathcal{M}$ , denoted by  $\hat{\partial}F(X)$ , is given by

$$(A.2) \quad \partial_R F(X) = \{\xi \in T_X \mathcal{M} : \langle \xi, V \rangle \leq F^\circ(X, V), \forall V \in T_X \mathcal{M}\}.$$

**Definition A.2.** ([42]) A function  $f$  is said to be regular at  $X \in \mathcal{M}$  along  $T_X \mathcal{M}$  if

- for all  $V \in T_X \mathcal{M}$ ,  $f'(X; V) = \lim_{t \downarrow 0} \frac{f(X+tV) - f(X)}{t}$  exists, and
- for all  $V \in T_X \mathcal{M}$ ,  $f'(X; V) = f^\circ(X; V)$ .

For a smooth function  $f$  over Riemannian submanifold, if the metric on the manifold is induced by the Euclidean inner product in the ambient space, then we know that  $\mathbf{grad} f(X) = \text{Proj}_{T_X \mathcal{M}} \nabla f(X)$ . Here  $\mathbf{grad} f$  denotes the Riemannian gradient of  $f$ , and  $\text{Proj}_{T_X \mathcal{M}}$  denotes the projection onto  $T_X \mathcal{M}$ . According to Lemma 5.1 in [42], for a regular function<sup>3</sup>  $F$ , we have  $\partial_R F(X) = \text{Proj}_{T_X \mathcal{M}}(\partial F(X))$ . Moreover, the function  $h(c(U))$  in problem (2.5) is weakly convex and thus is regular according to Lemma 5.1 in [42]. By Theorem 4.1 in [42], the first-order optimality condition of problem (2.5) is given by

$$(A.3) \quad 0 \in \text{Proj}_{T_U \mathcal{M}} \nabla c(U)^\top \partial h(c(U)) + \mathbf{grad} f(U).$$

**Definition A.3.** A point  $U \in \mathcal{M}$  is called a stationary point of problem (2.5) if it satisfies the first-order optimality condition (A.3).

**Definition A.4.** A retraction on an differentiable manifold  $\mathcal{M}$  is a smooth mapping  $\text{Retr}$  from the tangent bundle  $T\mathcal{M}$  onto  $\mathcal{M}$  satisfying the following two conditions (here  $\text{Retr}_X$  denotes the restriction of  $\text{Retr}$  onto  $T_X \mathcal{M}$ )

- $\text{Retr}_X(0) = X, \forall X \in \mathcal{M}$ , where 0 denotes the zero element of  $T_X \mathcal{M}$ .
- For  $X \in \mathcal{M}$ , it holds that

$$\lim_{T_X \mathcal{M} \ni \xi \rightarrow 0} \frac{\|\text{Retr}_X(\xi) - (X + \xi)\|_F}{\|\xi\|_F} = 0$$

The retraction onto the Euclidean space is simply the identity mapping:  $\text{Retr}_X(\xi) = X + \xi$ . Common retractions include the polar decomposition:

$$\text{Retr}_X^{\text{polar}}(\xi) = (X + \xi)(I_r + \xi^\top \xi)^{-1/2}$$

---

<sup>3</sup>See the definition in [42]. Convex function is regular and the addition of regular functions is regular. The generalized subdifferential of  $f(U)$  is the projection of its convex subdifferential.

the QR decomposition:

$$\text{Retr}_X^{QR} = \mathbf{qf}(X + \xi)$$

where  $\mathbf{qf}(A)$  is the  $Q$  factor of the QR factorization of  $A$ ; the Cayley transformation,

$$\text{Retr}_X^{\text{cayley}}(\xi) = \left(I_n - \frac{1}{2}W(\xi)\right)^{-1} \left(I_n + \frac{1}{2}W(\xi)\right)X$$

where  $W(\xi) = (I_n - \frac{1}{2}XX^\top)\xi X^\top - X\xi^\top(I_n - \frac{1}{2}XX^\top)$

**Lemma A.5.** [10] For all  $X \in \mathcal{M}$  and  $\xi \in \mathbb{T}_X\mathcal{M}$  there exist constants  $M_1 > 0$  and  $M_2 > 0$  such that the following two inequalities hold:

$$(A.4) \quad \|\text{Retr}_X(\xi) - X\|_F \leq M_1 \|\xi\|_F, \forall X \in \mathcal{M}, \xi \in \mathbb{T}_X\mathcal{M}$$

$$(A.5) \quad \|\text{Retr}_X(\xi) - (X + \xi)\|_F \leq M_2 \|\xi\|_F^2, \forall X \in \mathcal{M}, \xi \in \mathbb{T}_X\mathcal{M}.$$

**Lemma A.6.** The function  $h$  in (2.5) is  $L_h$ -Lipschitz continuous and the Jacobian  $\nabla c(x)$  is  $L_c$ -Lipschitz continuous, where  $L_h = n\lambda$  and  $L_c = 2$ .

*Proof.* Since  $h(Z) = \lambda\|Z\|_1$  where  $Z \in \mathbb{R}^{n \times n}$ , we immediately get that  $h$  is  $n\lambda$ -Lipschitz continuous. Secondly, observing that  $\nabla c(U)V = UV^\top + VU^\top$  for any  $V \in \mathbb{R}^{n \times k}$ , we have

$$\|\nabla c(U_1) - \nabla c(U_2)\|_{\text{op}} = \max_{\|V\|_F=1} \|(U_1 - U_2)V^\top + V(U_1 - U_2)^\top\|_F \leq 2\|U_1 - U_2\|_F.$$

Hence,  $\nabla c(x)$  is 2-Lipschitz continuous. ■

## Appendix B. Proofs.

**B.1. Convergence Analysis of ManPL (Algorithm 2.1).** Before we presents the result in ManPL, we need the following useful lemma in proximal linear algorithm.

**Lemma B.1.** [15] Under the assumptions on  $h$  and  $c$ , we have the following result:

$$(B.1) \quad -\frac{L_c L_h}{2} \|U_2 - U_1\|_F^2 \leq h(c(U_2)) - h(c(U_1) + \nabla c(U_1)(U_2 - U_1)) \leq \frac{L_c L_h}{2} \|U_2 - U_1\|_F^2$$

*Proof.* It follows form Lemma A.6 that

$$\begin{aligned} & \left| h(c(U_2)) - h(c(U_1) + \nabla c(U_1)(U_2 - U_1)) \right| \\ & \leq L_h \|c(U_2) - (c(U_1) + \nabla c(U_1)(U_2 - U_1))\|_F \\ & = L_h \left\| \int_0^1 (\nabla c(U_1 + t(U_2 - U_1)) - \nabla c(U_1))(U_2 - U_1) dt \right\|_F \\ & \leq L_h \int_0^1 \|\nabla c(U_1 + t(U_2 - U_1)) - \nabla c(U_1)\|_{\text{op}} \|U_2 - U_1\|_F dt \\ & \leq L_h L_c \left( \int_0^1 t dt \right) \|U_2 - U_1\|_F^2 = \frac{L_c L_h}{2} \|U_2 - U_1\|_F^2. \end{aligned}$$

14 ■

Now, we start to analyze the convergence and iteration complexity of our ManPL algorithm. The following lemma states that the minimizer of (2.9a) is a descent direction on the tangent space for the local model.

**Lemma B.2.** *Let  $V^k$  be the minimizer of (2.9a), the following holds for any  $\alpha \in [0, 1]$ , with any  $t > 0$ ,*

(B.2)

$$\langle \nabla f(U^k), \alpha V^k \rangle + \frac{1}{2t} \|\alpha V^k\|_F^2 + h(c(U^k) + \alpha \nabla c(U^k) V^k) - h(c(U^k)) \leq \frac{\alpha^2 - 2\alpha}{2t} \|V^k\|_F^2.$$

*Proof.* Since  $V^k$  is the minimizer of (2.9a), we will have for any  $\alpha \in [0, 1]$ :

$$\begin{aligned} & \langle \nabla f(U^k), \alpha V^k \rangle + \frac{1}{2t} \|\alpha V^k\|_F^2 + h(c(U^k) + \alpha \nabla c(U^k) V^k) \\ & \geq \langle \nabla f(U^k), V^k \rangle + \frac{1}{2t} \|V^k\|_F^2 + h(c(U^k) + \nabla c(U^k) V^k) \end{aligned}$$

which implies that

$$\begin{aligned} & (1 - \alpha) \langle \nabla f(U^k), V^k \rangle + \frac{1 - \alpha^2}{2t} \|V^k\|_F^2 + h(c(U^k) + \nabla c(U^k) V^k) \\ & - h(c(U^k) + \alpha \nabla c(U^k) V^k) \leq 0. \end{aligned}$$

Using the convexity of  $h$ , we have

$$\langle \nabla f(U^k), V^k \rangle + \frac{1 + \alpha}{2t} \|V^k\|_F^2 + h(c(U^k) + \nabla c(U^k) V^k) - h(c(U^k)) \leq 0$$

Letting  $\alpha \rightarrow 1$ , we get

$$\langle \nabla f(U^k), V^k \rangle + h(c(U^k) + \nabla c(U^k) V^k) - h(c(U^k)) \leq -\frac{1}{t} \|V^k\|_F^2.$$

Finally, from the convexity of  $h$  we get

$$\begin{aligned} & \langle \nabla f(U^k), \alpha V^k \rangle + \frac{1}{2t} \|\alpha V^k\|_F^2 + h(c(U^k) + \alpha \nabla c(U^k) V^k) - h(c(U^k)) \\ & \leq \alpha \left( \langle \nabla f(U^k), V^k \rangle + h(c(U^k) + \nabla c(U^k) V^k) - h(c(U^k)) \right) + \frac{\alpha^2}{2t} \|V^k\|_F^2 \\ & \leq \frac{\alpha^2 - 2\alpha}{2t} \|V^k\|_F^2, \end{aligned}$$

which completes the proof. ■

The following lemma suggests that the new point  $U^{k+1} = \text{Retr}_{U^k}(\alpha V^k)$  has a lower function value.

**Lemma B.3.** *Given any  $t > 0$ , consider  $V^k$  is the optimal solution of (2.9a). Denote  $U^{k+1} = \text{Retr}_{U^k}(\alpha V^k)$ , there exists a constant  $\bar{\alpha} > 0$  such that*

$$(B.3) \quad F(U^{k+1}) - F(U^k) \leq -\frac{\alpha}{2} \|V^k\|_F^2, \quad \forall 0 \leq \alpha \leq \min\{1, \bar{\alpha}\}.$$

*Proof.* We will prove by induction. Denote  $U_+^k = U^k + \alpha V^k$ . For  $k = 0$ , by using the convexity of  $h$  and Lipchitz continuity of  $c$ , we can show that:

$$\begin{aligned}
& h(c(U^{k+1})) - h(c(U^k) + \alpha \nabla c(U^k) V^k) \\
&= h(c(U^{k+1})) - h(c(U^k) + \nabla c(U^k)(U^{k+1} - U^k)) \\
&\quad + h(c(U^k) + \nabla c(U^k)(U^{k+1} - U^k)) - h(c(U^k) + \nabla c(U^k)(U_+^k - U^k)) \\
\text{(B.4)} \quad & \stackrel{\text{(B.1)}}{\leq} \frac{L_h L_c}{2} \|U^{k+1} - U^k\|_F^2 + L_h \|\nabla c(U^k)(U^{k+1} - U_+^k)\|_F \\
& \stackrel{\text{(A.4)}}{\leq} \frac{\alpha^2 L_h L_c}{2} M_1^2 \|V^k\|_F^2 + L_h \|\nabla c(U^k)(U^{k+1} - U_+^k)\|_F \\
& \stackrel{\text{(A.5)}}{\leq} \frac{\alpha^2 L_c L_h}{2} M_1^2 \|V^k\|_F^2 + L_h L_c M_2 \alpha^2 \|V^k\|_F^2 = \left(\frac{1}{2} M_1^2 + M_2\right) L_c L_h \alpha^2 \|V^k\|_F^2.
\end{aligned}$$

Since  $\nabla f(X)$  is  $L_f$  Lipschitz continuous, we obtain

$$\begin{aligned}
f(U^{k+1}) - f(U^k) &\leq \langle \nabla f(U^k), U^{k+1} - U^k \rangle + \frac{L_f}{2} \|U^{k+1} - U^k\|_F^2 \\
&= \langle \nabla f(U^k), U^{k+1} - U_+^k + U_+^k - U^k \rangle + \frac{L_f}{2} \|U^{k+1} - U^k\|_F^2 \\
\text{(B.5)} \quad & \stackrel{\text{(A.5)}}{\leq} M_2 \|\nabla f(U^k)\|_F \|\alpha V^k\|_F^2 + \alpha \langle \nabla f(U^k), V^k \rangle + \frac{M_1^2 L_f}{2} \|\alpha V^k\|_F^2 \\
& \leq c_0 \alpha^2 \|V^k\|_F^2 + \alpha \langle \nabla f(U^k), V^k \rangle,
\end{aligned}$$

where  $c_0 = M_2 G + \frac{M_1^2 L_f}{2}$  and  $G = \max_{U \in \mathcal{M}} \|\nabla f(U)\|_F$ .

Now we need to show that the value of objective function converges. It follows that

$$\begin{aligned}
& F(U^{k+1}) - F(U^k) \\
& \stackrel{\text{(B.5)}}{\leq} \alpha \langle \nabla f(U^k), V^k \rangle + c_0 \alpha^2 \|V^k\|_F^2 + h(c(U^{k+1})) - h(c(U^k) + \alpha \nabla c(U^k) V^k) \\
& \quad + h(c(U^k) + \alpha \nabla c(U^k) V^k) - h(c(U^k)) \\
& \stackrel{\text{(B.4)}}{\leq} \alpha \langle \nabla f(U^k), V^k \rangle + c_0 \alpha^2 \|V^k\|_F^2 + \left(\frac{1}{2} M_1^2 + M_2\right) L_c L_h \alpha^2 \|V^k\|_F^2 \\
& \quad + \alpha \left( h(c(U^k) + \nabla c(U^k) V^k) - h(c(U^k)) \right) \\
& \stackrel{\text{(B.2)}}{\leq} \left[ \left( c_0 + \left( \frac{1}{2} M_1^2 + M_2 \right) L_c L_h \right) \alpha^2 - \frac{\alpha}{t} \right] \|V^k\|_F^2.
\end{aligned}$$

Letting  $\bar{\alpha} = \frac{1}{2 \left( c_0 + \left( \frac{1}{2} M_1^2 + M_2 \right) L_c L_h \right) t}$ , we get that for any  $0 \leq \alpha \leq \min\{1, \bar{\alpha}\}$ ,

$$\text{(B.6)} \quad F(\text{Retr}_{U^k}(\alpha V^k)) - F(U^k) \leq -\frac{\alpha}{2t} \|V^k\|_F^2.$$

Thus, the result (B.3) holds for  $k = 0$ . Using induction, we can show that (B.3) holds for all  $k \geq 1$ . The proof is completed.  $\blacksquare$



**Definition B.4.** Given any  $t > 0$ ,  $U^k$  is called an  $\epsilon$ -stationary point of (2.5), if the exact solution  $V^k$  to (2.9a) satisfies  $\|V^k/t\|_F \leq \epsilon$ .

**Lemma B.5.** If  $V^k = 0$ , then  $U^k$  is a stationary point of problem (2.5).

*Proof.* Consider the optimality conditions for the subproblem of ManPL is given by:

$$0 \in \text{Proj}_{T_{U^k}\mathcal{M}} \nabla c(U^k)^\top \partial h(c(U^k) + \nabla c(U^k)V^k) + \frac{1}{t}V^k + \mathbf{grad} f(U^k),$$

where  $V^k \in T_{U^k}\mathcal{M}$ . If  $V^k = 0$ , it follows that

$$0 \in \text{Proj}_{T_{U^k}\mathcal{M}} \nabla c(U^k)^\top \partial h(c(U^k)) + \mathbf{grad} f(U^k)$$

which is the first-order optimality condition of (2.5). ■

*Proof of Theorem 2.1.* By using Lemma B.3, the claimed result directly follows from the proof of [10, Theorem 5.5]. We omit the details for brevity. ■

## B.2. Convergence Analysis of AManPL (Algorithm 3.1).

**Lemma B.6.** (Sufficient decrease in  $w$  subproblem) By following the updating scheme (3.4) for  $w$  subproblem, we have

$$(B.7) \quad \bar{F}(U^{k+1}, w^{k+1}) - \bar{F}(U^{k+1}, w^k) \leq -\frac{\rho}{2} \|w^{k+1} - w^k\|_2^2.$$

*Proof.* This follows from the  $\rho$ -strong convexity of the objective function of (3.3). ■

**Lemma B.7.** Let  $V^k$  be the optimal solution of (3.9a) and  $t > 0$ . There exists  $\hat{\alpha} > 0$  such that for any  $0 \leq \alpha \leq \min\{1, \hat{\alpha}\}$  and  $U^{k+1} = \text{Retr}_{U^k}(\alpha V^k)$ ,

$$(B.8) \quad \bar{F}(U^{k+1}, w^{k+1}) - \bar{F}(U^k, w^k) \leq -\left(\frac{\alpha}{2t} \|V^k\|_F^2 + \frac{\rho}{2} \|w^{k+1} - w^k\|_2^2\right).$$

*Proof.* Firstly we show that the subproblem (3.8) admits the same form of (2.5). That is, we show that  $\mathbf{f}(U, w^k) = \sum_{\ell=1}^T w_\ell^k \langle L^{(\ell)}, UU^\top \rangle$  is smooth and its gradient is Lipschitz continuous. Once we prove this, then the remaining steps will follow the proof of lemma B.3. Note that for any  $w \in \mathbb{R}^T$ , we have:

$$\begin{aligned} \|\nabla_U \mathbf{f}(U_1, w^k) - \nabla_U \mathbf{f}(U_2, w^k)\|_F &= \left\| 2 \sum_{\ell=1}^T w_\ell^k L^{(\ell)} (U_1 - U_2) \right\|_F \\ &\leq 2 \sum_{\ell=1}^T w_\ell^k \|L^{(\ell)}\|_2 \|U_1 - U_2\|_F \leq 2 \|U_1 - U_2\|_F, \end{aligned}$$

where we use the fact that  $\|L^{(\ell)}\|_2 = 1$  for every  $\ell$  (followed by the property of affinity matrix). This implies that for fixed  $w^k$ ,  $f(\cdot, w^k)$  is smooth and its gradient is Lipschitz continuous with Lipschitz constant  $L_f = 2$ . Now we can use Lemma B.3 and let  $\hat{\alpha} = \frac{1}{2\left(c_1 + \left(\frac{1}{2}M_1^2 + M_2\right)L_c L_h\right)t}$ ,

where  $c_1 = M_2 G_1 + \frac{L_f M_1^2}{2}$  and  $G_1 = \max_{U \in \mathcal{M}, 1 \geq w \geq 0} \|\nabla \mathbf{f}(U, w)\|_F$ , where  $M_1$  and  $M_2$  are constants defined in [Lemma A.5](#). From [Lemma B.3](#) we get that for any  $0 \leq \alpha \leq \min\{1, \hat{\alpha}\}$ ,

$$\bar{F}(\text{Retr}_{U^k}(\alpha V^k), w^k) - \bar{F}(U^k, w^k) \leq -\frac{\alpha}{2t} \|V^k\|_F^2,$$

which together with [\(B.7\)](#) yields the desired result [\(B.8\)](#). ■

**Lemma B.8.** *For given  $(U^k, w^k)$  generated from the  $k$ -th iteration of AManPL, if  $V^k = 0$ , where  $V^k$  is the optimal solution to [\(3.9a\)](#), then  $(U^k, w^k)$  is a stationary point of problem [\(1.3\)](#).*

*Proof.* Since  $V^k = 0$ , the optimality condition of [\(3.9a\)](#) implies that

$$(B.9) \quad 0 \in \text{Proj}_{\mathbb{T}_{U^k} \mathcal{M}} \left( 2 \sum_{\ell=1}^T w_\ell^k L^{(\ell)} U^k + \nabla c(U^k)^\top \partial h(c(U^k)) \right).$$

Moreover, the optimality condition to [\(3.10\)](#) implies that

$$(B.10) \quad 0 \in c_\ell + \rho(\log(w_\ell^k) + 1) + \partial_\ell \mathbb{I}(w^k),$$

where  $c_\ell = \langle U^k U^{k\top}, L^{(\ell)} \rangle$ ,  $\ell = 1, \dots, T$ , and  $\mathbb{I}(w)$  denotes the indicator function of the probability simplex constraint  $\mathcal{S} := \{w \mid \sum_{\ell=1}^T w_\ell = 1, w_\ell \geq 0, \ell = 1, \dots, T\}$ , i.e.,  $\mathbb{I}(w) = 0$  if  $w \in \mathcal{S}$ , and  $\mathbb{I}(w) = +\infty$  otherwise. Moreover, since

$$\partial_R(h(c(U)), \mathbb{I}(w)) = \text{Proj}_{\mathbb{T}_U \mathcal{M}} \left( \nabla c(U)^\top \partial h(c(U)) \right) \times \partial \mathbb{I}(w),$$

the first-order optimal condition of [\(1.3\)](#) is given by

$$(B.11) \quad \begin{aligned} 0 &\in \text{Proj}_{\mathbb{T}_U \mathcal{M}} \left( 2 \sum_{\ell=1}^T w_\ell L^{(\ell)} U + \nabla c(U)^\top \partial h(c(U)) \right) \\ 0 &\in \langle L^{(\ell)}, U U^\top \rangle + \rho(\log(w_\ell) + 1) + \partial_\ell \mathbb{I}(w), \quad \forall \ell. \end{aligned}$$

From [\(B.9\)](#) and [\(B.10\)](#) we know that  $(U^k, w^k)$  satisfies the optimality condition [\(B.11\)](#). Therefore  $(U^k, w^k)$  is a stationary point of [\(1.3\)](#). ■

Since for the  $w$ -subproblem [\(3.3\)](#), one always has [\(B.10\)](#). This motivates us to define the following  $\epsilon$ -stationarity.

**Definition B.9.** *We call a point  $(U^k, w^k)$  an  $\epsilon$ -stationary point of problem [\(1.3\)](#) if*

$$\left\| V^k / t \right\|_F \leq \epsilon,$$

where  $V_k$  is the optimal solution to [\(3.9a\)](#).

*Proof of Theorem 3.1.* Since the feasible region of (1.3), there exists a convergent subsequence of  $\{U^k, w^k\}$ . Let us denote a limiting point as  $\{U^*, w^*\}$ . By using Lemma B.7, we have

$$\lim_{k \rightarrow \infty} \left\| V^k/t \right\|_F^2 + \left\| \rho(w^{k+1} - w^k) \right\|_2^2 = 0.$$

Note that the function  $h(c(U) + \nabla c(U)V)$  is convex with respect to  $V$ , therefore, taking limit for (B.9) and (B.10) gives

$$0 \in \text{Proj}_{T_{U^*} \mathcal{M}} \left( 2 \sum_{\ell=1}^T w_\ell^* L^{(\ell)} U^* + \nabla c(U^*)^\top \partial h(c(U^*)) \right)$$

and

$$0 \in c_\ell^* + \rho(\log(w_\ell^*) + 1) + \partial_\ell \mathbb{I}(w^*), \quad \ell = 1, \dots, T.$$

This suggests that  $(U^*, w^*)$  is the stationary point. The proof of the first statement is finished.

Secondly, given  $N \geq \frac{2t\hat{\alpha}\gamma(\bar{F}(U^0, w^0) - \bar{F}^*)}{\epsilon^2}$  it follows from Lemma B.7 that

$$\min_{k=1, \dots, N} \left\| V^k/t \right\|_F^2 \leq \epsilon^2.$$

The proof is completed. ■

## REFERENCES

- [1] P.-A. ABSIL, R. MAHONY, AND R. SEPULCHRE, *Optimization Algorithms on Matrix Manifolds*, Princeton University Press, Princeton, NJ, 2008.
- [2] T. BENDORY, Y. C. ELDAR, AND N. BOUMAL, *Non-convex phase retrieval from STFT measurements*, IEEE Transactions on Information Theory, (2018).
- [3] N. BOUMAL, *Nonconvex phase synchronization*, SIAM Journal on Optimization, 26 (2016), pp. 2355–2377.
- [4] N. BOUMAL AND P.-A. ABSIL, *Rtrmc: A riemannian trust-region method for low-rank matrix completion*, in Advances in neural information processing systems, 2011, pp. 406–414.
- [5] F. BUETTNER, K. N. NATARAJAN, F. P. CASALE, V. PROSERPIO, A. SCIALDONE, F. J. THEIS, S. A. TEICHMANN, J. C. MARIONI, AND O. STEGLE, *Computational analysis of cell-to-cell heterogeneity in single-cell rna-sequencing data reveals hidden subpopulations of cells*, Nature biotechnology, 33 (2015), p. 155.
- [6] V. CHARISOPOULOS, Y. CHEN, D. DAVIS, M. DIAZ, L. DING, AND D. DRUSVYATSKIY, *Low-rank matrix recovery with composite optimization: Good conditioning and rapid convergence*, <https://arxiv.org/pdf/1904.10020.pdf>, (2019).
- [7] V. CHARISOPOULOS, D. DAVIS, M. DÍAZ, AND D. DRUSVYATSKIY, *Composite optimization for robust blind deconvolution*, arXiv preprint arXiv:1901.01624, (2019).
- [8] S. CHEN, Z. DENG, S. MA, AND A. M.-C. SO, *Manifold proximal point algorithms for dual principal component pursuit and orthogonal dictionary learning*, in Proceedings of the 2019 Asilomar Conference on Signals, Systems, and Computers., 2019.
- [9] S. CHEN, Z. DENG, S. MA, AND A. M.-C. SO, *Manifold proximal point algorithms for dual principal component pursuit and orthogonal dictionary learning*, arXiv:2005.02356, (2020).
- [10] S. CHEN, S. MA, A. M.-C. SO, AND T. ZHANG, *Proximal gradient method for manifold optimization*, arXiv preprint arXiv:1811.00980, (2018).
- [11] S. CHEN, S. MA, L. XUE, AND H. ZOU, *An alternating manifold proximal gradient method for sparse PCA and sparse CCA*, INFORMS Journal on Optimization, in press, (2020).

- [12] A. CHERIAN AND S. SRA, *Riemannian dictionary learning and sparse coding for positive definite matrices*, IEEE Transactions on Neural Networks and Learning Systems, 28 (2017), pp. 2859–2871.
- [13] F. R. CHUNG AND F. C. GRAHAM, *Spectral Graph Theory*, American Mathematical Society, 1997.
- [14] Q. DENG, D. RAMSKÖLD, B. REINIUS, AND R. SANDBERG, *Single-cell rna-seq reveals dynamic, random monoallelic gene expression in mammalian cells*, Science, 343 (2014), pp. 193–196.
- [15] D. DRUSVYATSKIY AND C. PAQUETTE, *Efficiency of minimizing compositions of convex functions and smooth maps*, Mathematical Programming, (2018), pp. 1–56.
- [16] D. DUA AND C. GRAFF, *UCI machine learning repository*, 2017, <http://archive.ics.uci.edu/ml>.
- [17] J. C. DUCHI AND F. RUAN, *Solving (most) of a set of quadratic equalities: Composite optimization for robust phase retrieval*, arXiv preprint arXiv:1705.02356, (2017).
- [18] J. C. DUCHI AND F. RUAN, *Stochastic methods for composite and weakly convex optimization problems*, SIAM Journal on Optimization, 28 (2018), pp. 3229–3259.
- [19] O. P. FERREIRA AND P. R. OLIVEIRA, *Subgradient algorithm on Riemannian manifolds*, Journal of Optimization Theory and Applications, 97 (1998), pp. 93–104.
- [20] J. FRIEDMAN, T. HASTIE, AND R. TIBSHIRANI, *The Elements of Statistical Learning*, Springer Series in Statistics New York, 2001.
- [21] P. GROHS AND S. HOSSEINI,  $\varepsilon$ -subgradient algorithms for locally lipschitz functions on riemannian manifolds, Advances in Computational Mathematics, 42 (2016), pp. 333–360.
- [22] S. HOSSEINI AND M. POURYAYEVALI, *Generalized gradients and characterization of epi-lipschitz sets in riemannian manifolds*, Nonlinear Analysis: Theory, Methods & Applications, 74 (2011), pp. 3884–3895.
- [23] S. HOSSEINI AND A. USCHMAJEV, *A Riemannian gradient sampling algorithm for nonsmooth optimization on manifolds*, SIAM Journal on Optimization, 27 (2017), pp. 173–189.
- [24] V. Y. KISELEV, T. S. ANDREWS, AND M. HEMBERG, *Challenges in unsupervised clustering of single-cell rna-seq data*, Nature Reviews Genetics, (2019), p. 1.
- [25] A. S. LEWIS AND S. J. WRIGHT, *A proximal method for composite minimization*, Mathematical Programming, 158 (2016), pp. 501–546.
- [26] X. LI, S. CHEN, Z. DENG, Q. QU, Z. ZHU, AND A. M.-C. SO, *Weakly convex optimization over stiefel manifold using riemannian subgradient-type methods*, <https://arxiv.org/abs/1911.05047>, (2019).
- [27] H. LIU, M.-C. YUE, AND A. M.-C. SO, *On the estimation performance and convergence rate of the generalized power method for phase synchronization*, SIAM Journal on Optimization, 27 (2017), pp. 2426–2446.
- [28] C. LU, J. FENG, Z. LIN, AND S. YAN, *Nonconvex sparse spectral clustering by alternating direction method of multipliers and its convergence analysis*, in Thirty-Second AAAI Conference on Artificial Intelligence, 2018.
- [29] C. LU, S. YAN, AND Z. LIN, *Convex sparse spectral clustering: Single-view to multi-view*, IEEE Transactions on Image Processing (TIP), 25 (2016), pp. 2833–2843.
- [30] L. V. D. MAATEN AND G. HINTON, *Visualizing data using t-sne*, Journal of Machine Learning Research, 9 (2008), pp. 2579–2605.
- [31] A. Y. NG, M. I. JORDAN, AND Y. WEISS, *On spectral clustering: Analysis and an algorithm*, in Advances in neural information processing systems, 2002, pp. 849–856.
- [32] S. PARK AND H. ZHAO, *Spectral clustering based on learning similarity matrix*, Bioinformatics, 34 (2018), pp. 2069–2076.
- [33] A. A. POLLEN, T. J. NOWAKOWSKI, J. SHUGA, X. WANG, A. A. LEYRAT, J. H. LUI, N. LI, L. SZPANKOWSKI, B. FOWLER, P. CHEN, ET AL., *Low-coverage single-cell mrna sequencing reveals cellular heterogeneity and activated signaling pathways in developing cerebral cortex*, Nature biotechnology, 32 (2014), p. 1053.
- [34] A. SCHLITZER, V. SIVAKAMASUNDARI, J. CHEN, H. R. B. SUMATOH, J. SCHREUDER, J. LUM, B. MALLERET, S. ZHANG, A. LARBI, F. ZOLEZZI, ET AL., *Identification of cdc1-and cdc2-committed dc progenitors reveals early lineage priming at the common dc progenitor stage in the bone marrow*, Nature immunology, 16 (2015), p. 718.
- [35] J. SHI AND J. MALIK, *Normalized cuts and image segmentation*, IEEE Transactions on Pattern Analysis and Machine Intelligence, 22 (2000), pp. 888–905.
- [36] J. SUN, Q. QU, AND J. WRIGHT, *Complete dictionary recovery over the sphere i: Overview and the*

- geometric picture*, IEEE Transactions on Information Theory, 63 (2017), pp. 853–884.
- [37] J. SUN, Q. QU, AND J. WRIGHT, *A geometrical analysis of phase retrieval*, Foundations of Computational Mathematics, 18 (2018), pp. 1131–1198.
- [38] D. T. TING, B. S. WITTNER, M. LIGORIO, N. V. JORDAN, A. M. SHAH, D. T. MIYAMOTO, N. ACETO, F. BERSANI, B. W. BRANNIGAN, K. XEGA, ET AL., *Single-cell rna sequencing identifies extracellular matrix gene expression by pancreatic circulating tumor cells*, Cell reports, 8 (2014), pp. 1905–1918.
- [39] B. TREUTLEIN, D. G. BROWNFIELD, A. R. WU, N. F. NEFF, G. L. MANTALAS, F. H. ESPINOZA, T. J. DESAI, M. A. KRASNOW, AND S. R. QUAKE, *Reconstructing lineage hierarchies of the distal lung epithelium using single-cell rna-seq*, Nature, 509 (2014), p. 371.
- [40] B. WANG, S. MA, AND L. XUE, *Riemannian stochastic proximal gradient methods for nonsmooth optimization over the Stiefel manifold*, <https://arxiv.org/pdf/2005.01209.pdf>, (2020).
- [41] B. WANG, D. RAMAZZOTTI, L. DE SANO, J. ZHU, E. PIERSON, AND S. BATZOGLOU, *Simlr: a tool for large-scale single-cell analysis by multi-kernel learning*, bioRxiv, (2017), p. 118901.
- [42] W. H. YANG, L.-H. ZHANG, AND R. SONG, *Optimality conditions for the nonlinear programming problems on riemannian manifolds*, Pacific Journal of Optimization, 10 (2014), pp. 415–434.
- [43] H. ZOU AND L. XUE, *A selective overview of sparse principal component analysis*, Proceedings of the IEEE, 106 (2018), pp. 1311–1320.